Nano Today 33 (2020) 100873

Contents lists available at ScienceDirect

Nano Today

journal homepage: www.elsevier.com/locate/nanotoday

Triboelectric-polarization-enhanced high sensitive ZnO UV sensor

Hu Li[a,b], Luming Zhao[a], Jianping Meng[a], Caofeng Pan[a], Yan Zhang[d], Yaming Zhang[d], Zhuo Liu[a,b], Yang Zou[a], Yubo Fan[b,***], Zhong Lin Wang[a,c,e,**], Zhou Li[a,c,e,*]

[a] CAS Center for Excellence in Nanoscience, Beijing Key Laboratory of Micro-Nano Energy and Sensor, Beijing Institute of Nanoenergy and Nanosystems, Chinese Academy of Sciences, Beijing, 100083, PR China
[b] Beijing Advanced Innovation Centre for Biomedical Engineering, Key Laboratory for Biomechanics and Mechanobiology of Ministry of Education, School of Biological Science and Medical Engineering, Beijing Advanced Innovation Centre for Biomedical Engineering, Beihang University, Beijing, 100083, PR China
[c] School of Nanoscience and Technology, University of Chinese Academy of Sciences, Beijing, 100049, PR China
[d] School of Physics, University of Electronic Science and Technology of China, Chengdu, 610054, PR China
[e] School of Materials Science and Engineering, Georgia Institute of Technology, Atlanta, GA, 30332-0245, United States

ARTICLE INFO

Article history:
Received 19 February 2020
Received in revised form 27 March 2020
Accepted 6 April 2020

Keywords:
Triboelectric voltage
Schottky barrier height
UV detection
Triboelectric nanogenerator

ABSTRACT

Ultraviolet (UV) detection is of important significance in protecting environment, human health and related scenarios. Schottky barrier height (SBH) plays a key role in determining the performance of UV sensors. Herein, triboelectric voltage was proposed to lower the SBH of zinc oxide nano/micro wire and silver paste (ZnO//Ag) UV sensor. SBH was flexibly lowered by different times of triboelectric voltage treatment. Greatly improved UV response was achieved based on Schottky-to-Schottky contact after lowering its SBH, its photoresponse rates were enhanced by 645 % at raising edge from 6.77 s to 1.05 s, and 716 % at falling edge from 2.72 s to 0.38 s. The on/off ratio was greatly increased from 590 to 10400. Based on these results, the triboelectric technology may provide new views for tuning performance of Schottky-junction-based sensors. The developed tunable ZnO//Ag sensor combined with triboelectric voltage opens up possibility for future high sensitive UV sensing systems.

Introduction

Visible-blind ultraviolet (UV) photodetector is widely used in many fields, such as equipment maintenance, space communication, flame sensing and environment protection [1–4]. The sensitive UV detection has an important influence on scientific research, human health and developing relevant countermeasures. The photoresponse performance of UV sensor greatly depends on material's intrinsic property and external regulation [5–9]. One-dimensional nanomaterials (e.g., nanowire, nanofiber, nanotube, etc.) are often used for photodetection due to their high surface-to-volume ratio, anisotropic transmission and transparent property [10–14]. Zinc oxide (ZnO) nano/microwire (NMW), as a typical wide-bandgap semiconductor, is suitable for detecting UV light because of its proper bandgap band (i.e., 3.7 eV) and large exciton binding energy (i.e., 60 meV) [10]. Schottky junction between metal and ZnO NMW is usually preferred for UV sensors owing to the sensitive current tuning effect of Schottky barrier height (SBH) [15,16], which is determined during the sensor preparation process [17]. An appropriate external intervention (e.g., piezoelectric effect) of the SBH can effectively improve the photoresponse performance (e.g., photoresponse rate and on/off ratio) of ZnO NMW-based UV sensors [18,19].

According to previous reports, electric field can affect the charge diffusion at the contact interface between metal and semiconductor [20,21], it means that this effect can be an alternative choice to regulate the SBH and further improve the UV sensing performance of Schottky-contact sensors. Considering that the maturing triboelectric technology can generate high voltage by external mechanical stimulation [22–25], it could be a desired voltage source to polarize the charges within the contact interface (or depletion region), and further tune the SBH of ZnO and silver paste (ZnO//Ag) and enhance its UV response sensitivity. Compared with commercial voltage source, triboelectric technology has many advantages, such as self-powered ability without external power source, safety of high voltage and low current, simplicity of whole device, and cheapness of constituent materials [26–28]. To verify above assumption,

* Corresponding author at: CAS Center for Excellence in Nanoscience, Beijing Key Laboratory of Micro-Nano Energy and Sensor, Beijing Institute of Nanoenergy and Nanosystems, Chinese Academy of Sciences, Beijing, 100083, PR China.
** Corresponding author at: School of Nanoscience and Technology, University of Chinese Academy of Sciences, Beijing, 100049, PR China.
*** Corresponding author.
E-mail addresses: yubofan@buaa.edu.cn (Y. Fan), zhong.wang@mse.gatech.edu (Z.L. Wang), zli@binn.cas.cn, lizhou@ucas.ac.cn (Z. Li).

https://doi.org/10.1016/j.nantod.2020.100873
1748-0132/

triboelectric voltage was used to treat the Schottky junction of ZnO//Ag.

The results showed that triboelectric voltage was effective to three types of metal-semiconductor contacts, including "Schottky-to-Ohmic" contact, "Ohmic-to-Ohmic" contact and "Schottky-to-Schottky" contact. After the treatment, the SBH can be effectively lowered, especially for "Schottky-to-Schottky" contact, its UV response performance was greatly improved. The photoresponse rates of "Schottky-to-Schottky" contact were enhanced by 645 % and 716 % at the raising edge and falling edge, respectively. The on/off ratio of photoresponse current was greatly increased from 590 to 10400. These results proved that the triboelectric voltage can be a simple and effective method for tuning SBH, which greatly enhances the sensing performance of Schottky junction-based sensors. For other related Schottky-junction-based sensors, this study is of significant reference value to achieve high sensitive detection of gas, biomolecules and other objects.

Results and discussion

Basic structure and performance of ZnO//Ag sensor

The primary electric properties of these ZnO//Ag sensors were measured in dark to avoid the influence of ambient light. Fig. 1a shows the photoresponse performance before and after treatment by triboelectric voltage under UV light. The friction materials and the basic working mechanism of triboelectric nanogenerator (TENG) were shown in Fig. S1 and S2 in Supporting information. Fig. 1b showed the corresponding equivalent circuit diagram of the whole experimental setup. TENG can generate a wide range of voltages, which were suitable for tuning SBH of ZnO//Ag sensor (Fig. S3). In this work, the rectified triboelectric voltage was about 200 V (Fig. S4), it was used to treat ZnO//Ag sensor. The actual voltage applied on ZnO//Ag sensor was about 22 V (Fig. 1d). The *I-V* and *lg I-V* curves (Fig. 1c and e) show that this ZnO//Ag sensor has near-symmetrical SBHs at its two ends. This "Schottky-to-Schottky" contact was used for sensitive UV detection in this experiment. In the following parts, three types of metal-semiconductor contacts were treated by the 200 V of triboelectric voltage, and the performance variation was studied in detail.

"Schottky-to-Ohmic" contact

A ZnO//Ag sensor with asymmetric contacts was firstly fabricated and treated by triboelectric voltage (Fig. 2). The typical asymmetric *I-V* curve in dark indicates the formation of asymmetric contacts between silver paste and ZnO NMW (Fig. 2a). The asymmetric *lg I-V* curve (inset in Fig. 2a) indicates asymmetric SBHs at its two ends. The I-V characteristics of one ZnO//Ag sensor with Schottky-to-Ohmic contact with and without UV illumination was shown in Fig. S5. After treating the sensor by triboelectric voltage for different times, the resultant *I-V* curves were recorded (Fig. 2b and e). The dark current values were greatly raised from 1.1 nA to 400 nA at + 2 V (Figs. 2b and S6a). The turn-on voltage decreased from 0.5 V to 0.15 V (Fig. S6b). Meanwhile, the dark current at −2 V was also raised from near zero to about 1.7 nA (Figs. 2e and S6c). The corresponding turn-on voltage decreased from 2 V to 1.14 V (Fig. S6d). The enhancement of dark current from −2 V to +2 V indicates that the SBHs of the sensor were lowered by the triboelectric voltage. The plot of *ln I* with the power law of $V^{1/4}$ showed an approximate linear trend (Fig. S7), which indicated that the current transport matched thermo-electronic emission [29,30].

With treatment times increased, the SBHs at two ends continuously decreased to a stable value, this result was consistent with the variation trend of dark current in Fig. 2b and e. After withdrawing triboelectric voltage, the *I-V* curves of ZnO//Ag sensor can gradually recover to approximate original state after about 8 h (Figs. 2c, f and S8). The UV sensor with "Ohmic-to-Ohmic" contact was also fabricated in this experiment. The detailed study was put in the supporting information for its insensitive UV response (Fig. S9).

Mechanism of tuning SBH by triboelectric polarization model

Previous study proved that a strong electric field generated by high voltage can drive oxygen vacancies to diffuse in ZnO [20]. The charges of oxygen vacancies at contact interface can effectively control the SBH of metal-semiconductor (M-S). The driving and generating process of oxygen vacancies has been well studied. The oxygen vacancies are driven to migrate along c-axis as interstitial ions due to the unidirectional pyroelectric field of devices [20,31]. Herein, we used the classical model to show the physical accumulation process of oxygen vacancies when the as-prepared ZnO//Ag sensor was treated by triboelectric voltage.

The I-V curves of metal-semiconductor-metal (M-S -M) junctions show obviously different properties because of different contact behaviors in different physical conditions [29,32], and the measured I-V characteristics of different M-S -M contact behaviors are usually greatly different. Additionally, studies have showed that both the SBHs at two ends of M-S -M junction decreased after the device was treated by macroscopic electric field [21]. For simplification, an ideal classic M-S -M model (one end is perfect contact) was selected, and the electric property is determined mainly by the forward voltage [29]. This simplified model was used to demonstrate the variety of interface characteristic when the sensor was treated by triboelectric voltage.

As shown in Fig. 3a, Schottky junction is formed at the contact interface of ZnO NMW and silver paste. Initially, oxygen vacancies are randomly distributed in ZnO NMW. Few oxygen vacancies existed near contact interface. SBH stays at high level. The initial SBH was denoted as Φ_{SB0}. After treatment by triboelectric voltage, the oxygen vacancies (positive charges) are driven by generated electric field towards the contact interface, and then accumulate at the contact interface (depletion region). The accumulation of positive charges causes the SBH decreases from Φ_{SB0} to Φ_{SB} (Fig. 3b). After withdrawing the triboelectric voltage, oxygen vacancies diffuse at the opposite direction and disappear slowly under internal electric field, and then the SBH arise again and recover to approximate initial state during the rest of time (Fig. 3c).

The built-in potential (φ_{bi}) of M-S contact model can be given by the following formula [33–36]:

$$\varphi_{bi} = \frac{q}{2\varepsilon_s}(N_A W_{D_p}^2 + \rho_{polar} W_{polar}^2 + N_D W_{D_n}^2) \quad (1)$$

where N_D and N_A represent the concentration of donor and acceptor, respectively. ρ_{polar} and W_{polar} represent the polarization charges density and distribution width of oxygen vacancies, respectively. The ρ_{polar} and W_{polar} are functions of time that are gradually built up as the triboelectric voltage is applied. W_{Dp} and W_{Dn} represent the widths of depletion region on p-type and n-type semiconductors. Here, N_A and W_{Dp} can be postulated to be zero because the ZnO NMW used in this study is n-type. The relationship of current and voltage can be given by [33]:

$$J = J_0 \exp\left(\frac{q^2 \rho_{polar} W_{polar}^2}{2\varepsilon_s kT}\right)\left[\exp\left(\frac{qV}{kT}\right) - 1\right] \quad (2)$$

where V represents the bias voltage, T and k are the temperature and Boltzmann constant, respectively. J_0 and ε_s are the saturation

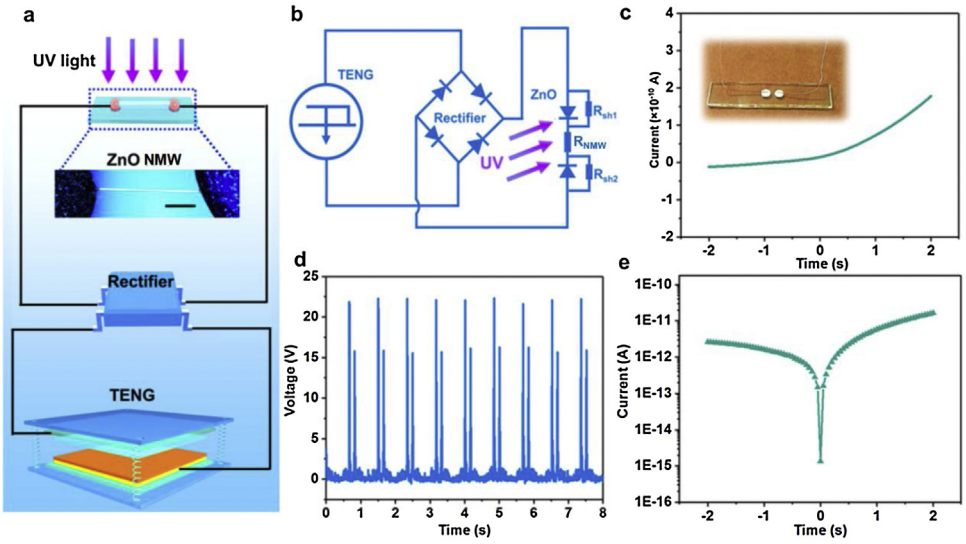

Fig. 1. Diagram of experiment setup and basic performance of TENG and ZnO//Ag UV sensor. (a) Setup diagram of tuning the SBH of ZnO//Ag UV sensor by triboelectric voltage for enhanced sensitive UV detection. Scale bar: 200 μm. The UV light was applied only after treatment by triboelectric voltage. (b) Corresponding circuit diagram of (a). (c, e) Typical *I-V* and *lg I-V* curves of ZnO//Ag UV sensor with "Schottky-to-Schottky" contact. The inset is an optical picture of ZnO//Ag UV sensor. (d) Triboelectric voltage applied on the two ends of ZnO//Ag UV sensor.

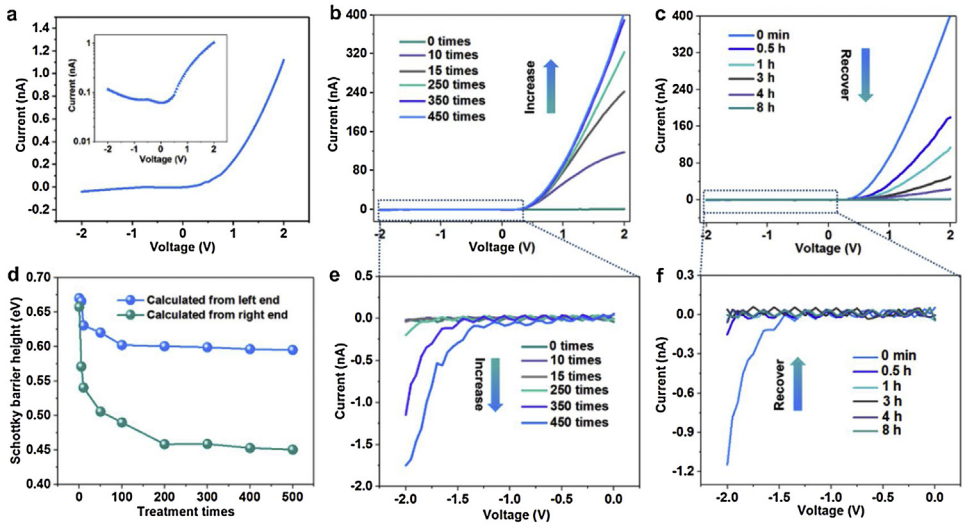

Fig. 2. Tuning SBH of ZnO//Ag UV sensor by triboelectric voltage. (a) Primary *I-V* curve with asymmetric SBHs in dark environment. The inset is lg *I-V* curve. (b) *I-V* curves after treatment for different times. (c) Recovery *I-V* curves after withdrawing triboelectric voltage for 8 h. (d) Calculated SBH values from the left end (−2 V to 0 V) and right end (0 V to +2 V) in (b). (e, f) Enlarged views of (b) and (c) from −2 V to 0 V, respectively.

current density and permittivity of the material, respectively. J_0 is given by [33]:

$$J_0 = \frac{q^2 D_n N_c}{kT}\sqrt{\frac{2qN_D(\varphi_{bio} - V)}{\varepsilon_s}}exp(-\frac{q\Phi_{SB0}}{kT}) \quad (3)$$

where N_c is the effective density of states at conduction band, D_n is electron diffusion coefficients, Φ_{SB0} is the Schottky barrier height and φ_{bi0} is the built-in potential without polarization charges. Many studies have investigated the effect of polarization charges on SBH [34,35]. After the polarization, the SBH of one dimensional M-S model will be decreased to Φ_{SB} [33]:

$$\Phi_{SB} = \Phi_{SB0} - \frac{q\rho_{polar}W_{polar}^2}{2\varepsilon_s} \quad (4)$$

"Schottky-to-Schottky" contact

SBH of metal-semiconductor contact greatly influences the carrier transport process. An appropriate tuning of SBHs can effectively promote the sensing performance of SHB-based sensors [37,38]. According to above results, triboelectric voltage was an efficient method to tune the SBH, which meant it can be used to improve the UV photoresponse performance. To verify this assumption, we fabricated ZnO//Ag sensors with two Schottky contacts on both ends (i.e., "Schottky-to-Schottky" contact). This sensor showed a very low dark current and a high photoresponse current under UV light without treatment by triboelectric voltage (Fig. 4a), which proved its suitability for UV detection. Then the sensor was treated by triboelectric voltage for different times (Fig. 4b) to lower its SBH. Compared with Fig. 4a, the photoresponse current at + 2 V was significantly enhanced from 93 nA to 527 nA after 20 times of treatment (Fig. 4b). The lowered SBH was consistent with the variation

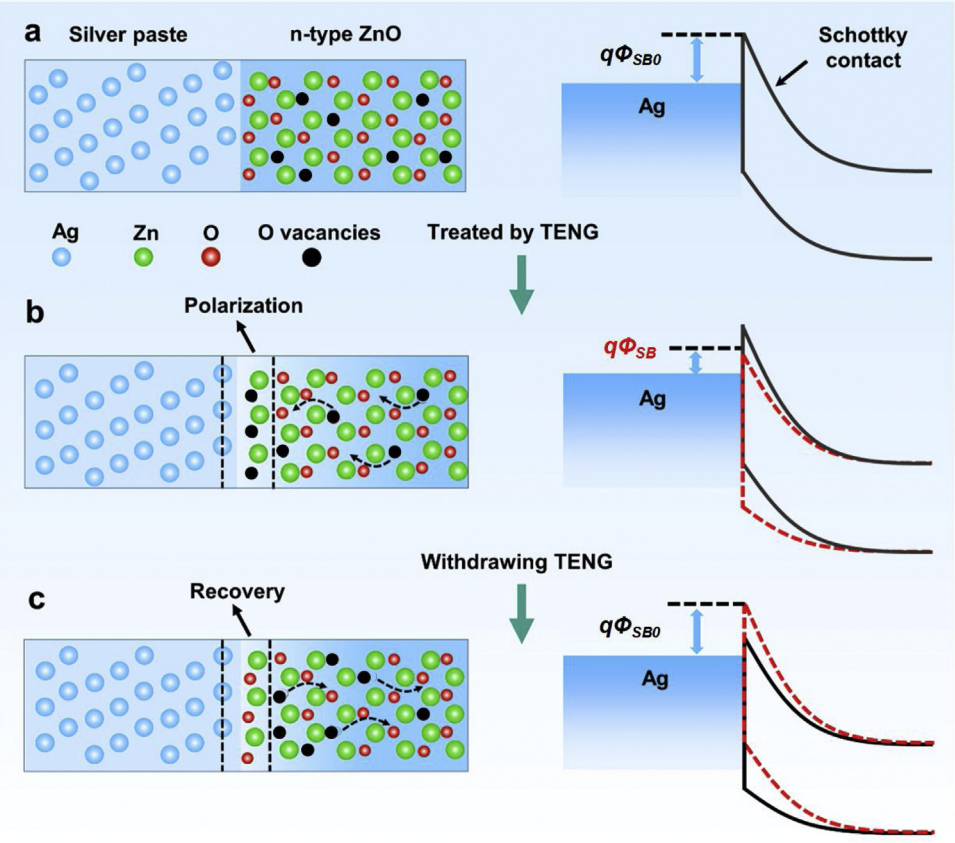

Fig. 3. Polarization model and SBH variation diagram. (a) Initial Schottky contact of ZnO//Ag. (b) Oxygen (O) vacancies are driven by triboelectric voltage, the positive charges are accumulated at the contact interface. After polarization, the SBH was decreased from Φ_{SB0} to Φ_{SB}. (c) After withdrawing triboelectric voltage, O vacancies diffuse slowly at the opposite direction, the accumulated positive charges vanish gradually, and the SBH recovers from Φ_{SB} to Φ_{SB0}.

trend of increased photoresponse current (Fig. 4b). SBH gradually decreased with the treatment times, the amount of lowered SBH reached to the maximum after 100 times of treatment (Fig. 4c), and the corresponding photoresponse current also reached to maximum value (Fig. S10). After withdrawing triboelectric voltage, the I-V curves of UV response gradually recovered to initial state within 6 h (Fig. S11). The response currents were recorded after treatment for different times from 0 to 300 times (Figs. 4d and S10).

As shown in Fig. 4d and g, when this ZnO//Ag sensor was exposed to UV light, the photoresponse current rose quickly first, then increased slowly to the maximum value, it took about 7 s. After turning off UV light, the photoresponse current fell off rapidly to the baseline, it took about 4 s, which proved that the primary ZnO//Ag sensor has good photoresponse performance at the moment of turning on/off the UV light. The on/off ratio reached to about 590 without treatment by triboelectric voltage. The rising edge and falling edge of the response curve have some degree of slope. After the sensor was treated for 50 times, the photoresponse current was tremendously raised near to tenfold. Additionally, the shape of photoresponse current curve is more similar to a rectangle (Fig. 4d and h). The photoresponse current rose rapidly to the maximum value and then fell fast to the baseline, this change indicated a largely improved photoresponse performance after the treatment by triboelectric voltage, including the response rate and on/off ratio. When the treatment times was more than 100, the UV photoresponse current achieved the optimal performance in terms of the sensitivity and on/off ratio. The response curves became smoother and more like a rectangle shape with vertical raising edges and falling edges. The on/off ratio reached up to about 10,400, which was much higher than that of primary ZnO NMWs without treatment. The improved photoresponse performance verified that the treatment by triboelectric voltage can be an effective method to tune the SBH and enhance the photoresponse performance of Schottky-junction-based UV sensor.

The photoresponse current was defined as the difference of photocurrent and dark current ($I_{uv} - I_{dark}$). The rising time was defined as the time from 10 % to 90 % of the maximum photocurrent. The falling time was defined as the time from 90 % to 10 % of the maximum photocurrent. The on/off ratio was defined as $R=(I_{uv} - I_{dark})/I_{dark}$ [39,40]. After the device was treated for 50 times, the maximum photoresponse current was greatly enhanced from 150 nA to about 1600 nA (Fig. 4d and h). Compared with the original sensor, the photoresponse current increased by 966.7 % after the treatment. The photoresponse current was further enhanced from 1600 nA to about 2660 nA after 100 times of treatment. The increase of photoresponse current reached up to 1673.3 % (Fig. 4d and i).

As shown in Fig. 4e, the photoresponse current and dark current were recorded as I_{max} and I_{min}, respectively. The I_{max} and I_{min} were plotted with treatment times. Both the I_{max} and I_{min} increased with the treatment times. The values of I_{max} and I_{min} reached to the maximum and kept stable after 100 times and 200 times of treatment, respectively. These results were consistent with the variation of SBH in Fig. 4c. Additionally, the photoresponse rate and recovery rate were also improved remarkably (Fig. 4f). Both the rising time and falling time were all obviously shortened. For the rising time, it was shortened from 6.77 s to 1.05 s, the sensitivity enhancement was 544.76 % in rising edge. For the falling time, it was shortened from 2.72 s to 0.38 s, the sensitivity enhancement was 615.79 % in falling edge. Compared with previous work, the sensing perfor-

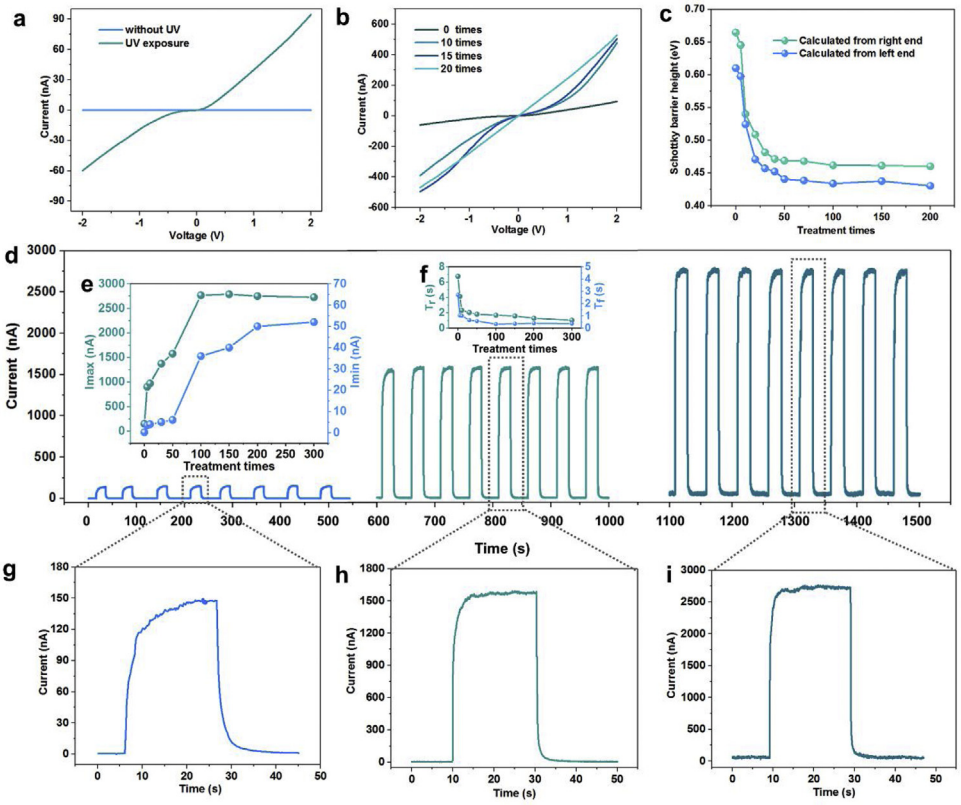

Fig. 4. Tuning the SBH of ZnO//Ag UV sensor with "Schottky-to-Schottky" contact by triboelectric voltage for enhanced UV detection. (a) Photoresponse curves without treatment by triboelectric voltage. (b) I-V curves with UV exposure after different times of treatment from 0 to 20 times. (c) SBH variation with treatment times under UV exposure. (d) Enhanced UV photoresponse after treatment by triboelectric voltage for different times. 0 times (left), 50 times (middle) and 100 times (right). (e) Photoresponse current and dark current variation with treatment times. (f) Rising time and falling time of the photoresponse current. (g-i) Enlarged view of photoresponse current in (d) reflecting the detailed shape change of current curve.

Table 1
Comparison of sensing performance of ZnO-based UV sensors.

Photodetector	Bias	Power density	On/off ratio	Rise time	Falling time	Ref.
Single ZnO NMW	2 V	0.32 mW cm^{-2}	1.04×10^4	1.05 s	0.38 s	This work
ZnO nanofiber	1 V	77.5 μW cm^{-2}	3.3×10^5	≈100 s	≈50 s	[7]
ZnO/CdO nanofiber	1 V	6.54 mW cm^{-2}	10^4–10^5	≈4 s	≈3 s	[12]
ZnO porous nanoparticle	5V	20 μW cm^{-2}	7.2×10^4	≈250 s	≈150 s	[10]
ZnO-SnO_2 nanofibers	10 V	0. 45 mW cm^{-2}	4.6×10^3	32.2 s	7.8 s	[41]
ZnO nanotetrapod network	2.4 V	15–20 mW cm^{-2}	4.5×10^3	≈67 ms	≈30 ms	[42]
ZnO-PbS nanofibers	10 V	7.02 mW cm^{-2}	$\approx 10^3$	9 s	2 s	[43]
ZnO-Cu nanowire	1 V	0.8 mW cm^{-2}	98	10.35 s	2 s	[44]
Sb-doped ZnO homojunction	3 V	60 mV cm^{-2}	33	15.2 s	20.3 s	[45]
Cu-doped ZnO homojunction	5 V	0.25 mW cm^{-2}	5.4	≈50 s	≈200 s	[46]
ZnO nanowire/graphene foam	5 V	1.3 mW cm^{-2}	–	9.5 s	38 s	[47]

mance of this ZnO//Ag UV sensor together with triboelectric voltage treatment is outstanding (Table 1).

Besides the SBH, the depletion layer width can also affect the UV detection sensitivity, which can be explained by the proposed energy band diagram in Fig. 5. The oxygen adsorption and desorption played a key role in regulating the UV detection of ZnO//Ag sensor. In dark condition, oxygen molecules adsorbed on nanowire surface and captured free electrons from ZnO as negatively charged ions, which formed a depletion layer with low conductivity near the nanowire surface (Fig. 5a):

$$O_2\,(g) + e^- \rightarrow O_2^-\,(ad) \tag{5}$$

Once ZnO NMW was exposed to UV light, electron-hole pairs were generated on nanowire surface, free holes were trapped by oxygen ions and induced the desorption of oxygen molecules from nanowire surface. The SBH decreases from Φ_1 to Φ_2 (Fig. 5b):

$$h^+ + O_2^-\,(ad) \rightarrow O_2(g) \tag{6}$$

Meanwhile, the desorption of oxygen molecules from depletion region near contact interface also resulted in the lowering of SBH and contributed to the increase of photoresponse current. With treatment by triboelectric voltage, the width of depletion region was broadened from W_{d1} to W_{d2} (Fig. 5a–c) according to the following equation [30]:

$$W_d = \sqrt{\frac{2\varepsilon_s}{qN_d}\left(\varphi_{bi0} - V - \frac{kT}{q}\right)} \tag{7}$$

where W_d represents the depletion region width, V is the applied triboelectric voltage on ZnO//Ag sensor, N_d is the doping concentration, q is the electron charge. The increase of the depletion region

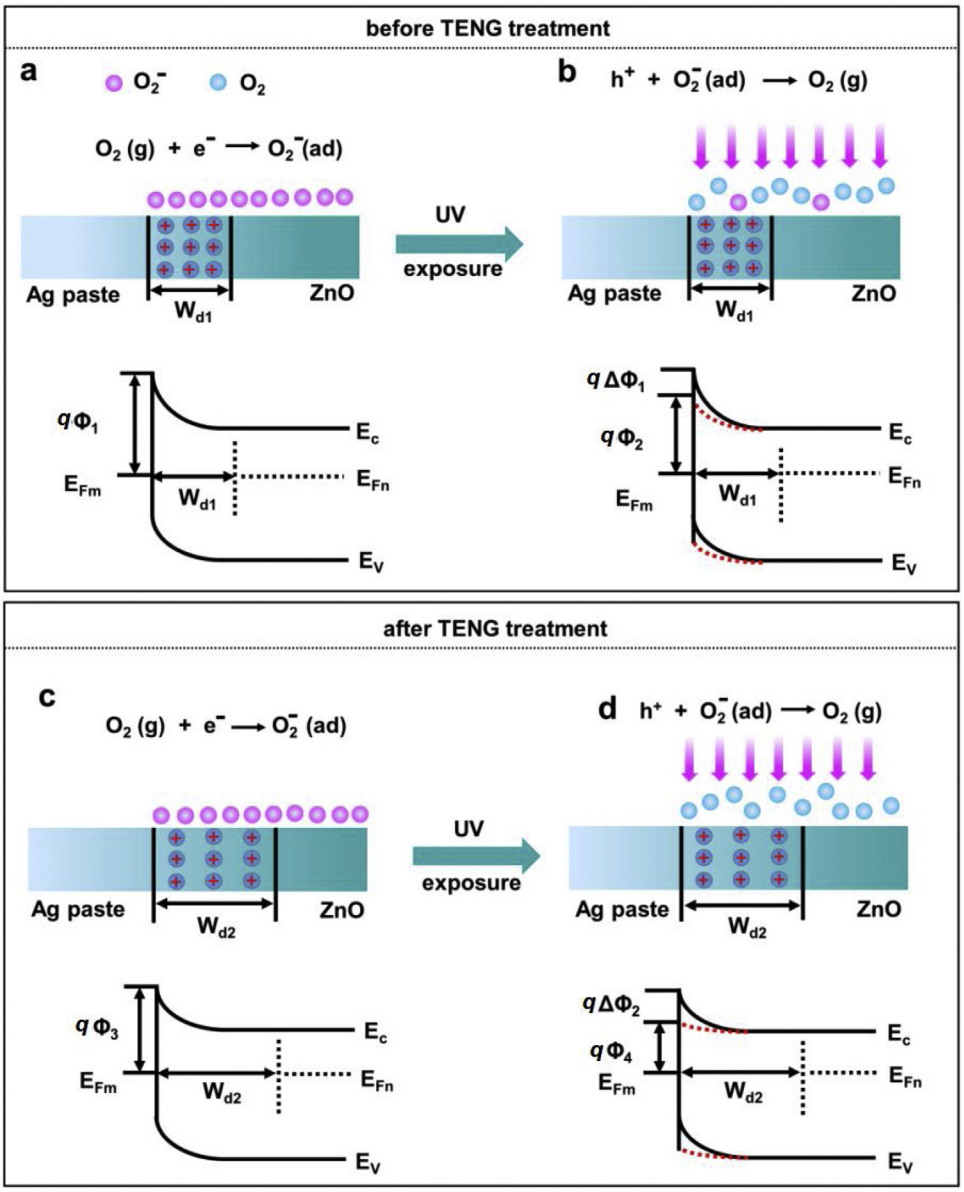

Fig. 5. Energy band diagram illustrating the variation of SBH and depletion region width (W_d) before and after treatment by triboelectric voltage. (a) Adsorption and (b) desorption of oxygen molecules before and after UV exposure without treatment by triboelectric voltage. (c) Adsorption and (d) desorption of oxygen molecules before and after UV exposure with treatment by triboelectric voltage.

width (W_d) means that the amount of adsorbed oxygen molecules was increased in the depletion region, it caused a larger amount of increased SBH from $\Delta\Phi_1$ to $\Delta\Phi_2$, which in turn affected the oxygen desorption amount under UV exposure. Once the sensor was exposed to UV light, the amount of lowered SBH will also be larger (i.e., $\Delta\Phi_2 > \Delta\Phi_1$) due to the oxygen desorption in the depletion region, which contributed to the increase of photoresponse current.

Conclusions

In summary, the SBHs of ZnO//Ag sensor were lowered successfully by triboelectric voltage, including Schottky-to-Ohmic contact, Ohmic-to-Ohmic contact and Schottky-to-Schottky contact. A polarization model was proposed that triboelectric voltage induced the polarization and drove the oxygen vacancy to accumulate at the contact interface, lowering the SBHs. High sensitive UV detection was achieved by lowering the SBH of Schottky-to-Schottky contact. Both the lowered SBH and broadened depletion region width contribute to enhancing the UV response performance. For "Schottky-to-Schottky" contact, the photoresponse rates were significantly enhanced by 645 % and 716 % at raising edge and falling edge, respectively. The on/off ratio of photoresponse current was greatly increased from 590 to 10400. This study may provide new thinking and avenue for tuning SBH of metal-semiconductor contact, which will greatly broaden the application scenarios of Schottky junction-based sensors, such as biomolecular detection, gas sensing, UV detection and other related objectives.

Experimental section

Synthesis of ZnO NMWs

ZnO NMWs in this experiment were synthesized by a vapor-liquid-solid growth method. An uniform mixture of ZnO nanopowder (1 g) and activated carbon powder (1 g) was put in an alumina boat, which was placed in the middle position of a tube

furnace in argon and oxygen atmosphere. A silicon substrate was deposited with a 5 nm of gold film on its surface. Then the substrate was put horizontally on the top of the alumina boat, and the gold surface faced down. The tube furnace was heated at 960 °C for 2 h. The gas flow rate of argon and oxygen were 60 sccm and 20 sccm, respectively. The as-synthesized NMWs were collected after the reaction was fully completed.

Fabrication of ZnO//Ag UV sensor

The ZnO//Ag UV sensor was fabricated by transferring and bonding an individual ZnO NMW laterally onto a precut sheet glass substrate, with its c-axis pointing to the source in the plane of the substrate. Moderate amounts of silver paste was used to fix the two ends of ZnO NMW, acting as the source and drain electrodes, respectively. Two leading wires were connected to the silver paste for electrical performance measurement.

Fabrication of TENG

To fabricate the TENG for treating ZnO//Ag UV sensor, two acrylic plates were shaped by a laser cutter to act as the supporting substrates (10 cm × 10 cm × 4 mm) of TENG. 2 mm thick 3 M tapes were adhered to the plates as spacers. At the four corners of acrylic plates, four holes were drilled for spring installation. A thin layer of copper film (thickness, 100 nm) was deposited on Kapton film to serve as back electrode. The prepared Kapton film with a dimension of 7.5 cm × 7.5 cm × 100 μm was fixed on one acrylic substrate. A precut polished aluminum foil with a dimension of 7.5 cm × 7.5 cm × 200 μm was fixed on another acrylic substrate. Then four coil springs were assembled on the top and bottom acrylic substrates. Finally, two leading wires were connected to the back electrode and aluminum foil for further electrical performance measurement.

Material characterization and electrical measurement

The microstructure of ZnO NMWs were characterized using scanning electron microscope (SEM; HITACHI, SU8020) and optical microscope (OM; Nikon, ECLIPSE LV100ND). The current-voltage characteristics of the as-fabricated UV sensors were measured by a semiconductor characterization system (KEITHLEY, 4200-SCS). The UV response characteristics of ZnO NMWs and electrical output of TENG were recorded using a digital oscilloscope (Teledyne LeCroy, HDO6104) and an electrometer (Keithley, 6517B). The wavelength and power of the used UV light were 365 nm and 0.32 mW/cm^2.

Author contributions

H. Li, L.M. Zhao and J.P. Meng contributed equally to this work. H. Li and L.M. Zhao conceived the idea and designed the experiment. Z. Li, Y.B. Fan and Z.L. Wang supervised the project. H. Li and L.M. Zhao fabricated the devices and performed the experiment. H. Li, L.M. Zhao and J.P. Meng analyzed the data, prepared the figures and wrote the manuscript. C.F. Pan provided the ZnO nano/microwires. Z. Liu and Y. Zou assisted in characterizing the materials. H. Li, L.M. Zhao, J.P. Meng, Y.M. Zhang and Y. Zhang proposed the theoretical models. All authors discussed and reviewed the manuscript.

Declaration of Competing Interest

All authors declare no conflict of interest of this manuscript.

Acknowledgements

The authors thank the support of National Key R&D Project from Minister of Science and Technology, China (2016YFA0202703), National Natural Science Foundation of China (Nos. 61875015, 31571006, 81601629, 21801019, 61501039, 11421202 and 11827803), the Beijing Natural Science Foundation (2182091), Science and Technology Planning Project of Guangdong Province</GN4>2018B030331001</GN4>, Beijing Council of Science and Technology (Z181100004418004) and the National Youth Talent Support Program.

References

[1] Z.Y. Li, L.C. Li, X.L. Jiang, J.L. Hu, Z.J. Zhang, W. Zhang, Energies 9 (2016) 369.
[2] Z.Y. Xu, B.M. Sadler, IEEE Commun. Mag. 46 (2008) 67–73.
[3] E.V. Gorokhov, A.N. Magunov, V.S. Feshchenko, A.A. Altukhov, Instrum. Exp. Tech. 51 (2008) 280–283.
[4] D.L. Giokas, A. Salvador, A. Chisvert, TrAC-Trend. Anal. Chem. 26 (2007) 360–374.
[5] L.D. Zhang, M. Fang, Nano Today 5 (2010) 128–142.
[6] A. Elzatahry, F.X. Bu, M.M. Zagho, Y. Ibrahim, B. Ma, D.Y. Zhao, Nano Today 30 (2020) 100803.
[7] X. Liu, L.L. Gu, Q.P. Zhang, J.Y. Wu, Y.Z. Long, Z.Y. Fan, Nat. Commun. 5 (2014) 4007.
[8] Z.N. Wang, R.M. Yu, C.F. Pan, Z.L. Li, J. Yang, F. Yi, Z.L. Wang, Nat. Commun. 6 (2015) 8401.
[9] Y. Qin, X.D. Wang, Z.L. Wang, Nature 451 (2008) 809.
[10] N. Nasiri, R.H. Bo, F. Wang, L. Fu, A. Tricoli, Adv. Mater. 27 (2015) 4336–4343.
[11] H.Y. Chen, H. Liu, Z.M. Zhang, K. Hu, X.S. Fang, Adv. Mater. 28 (2016) 403–433.
[12] Z. Zheng, L. Gan, H.Q. Li, Y. Ma, Y. Bando, D. Golberg, T.Y. Zhai, Adv. Funct. Mater. 25 (2015) 5885–5894.
[13] Z.K. Liu, S.Y. Liu, W.Z. Wu, C.R. Liu, Nanoscale 11 (2019) 2617–2623.
[14] H. Li, H. Ouyang, M. Yu, N. Wu, X. Wang, W. Jiang, Z. Liu, J. Tian, Y. Jin, H. Feng, Y. Fan, Z. Li,Small 13 (2017), 1603642.
[15] J. Zhou, Y.D. Gu, Y.F. Hu, W.J. Mai, P.-H. Yeh, G. Bao, A.K. Sood, D.L. Polla, Z.L. Wang,Appl. Phys. Lett. 94 (2009), 191103.
[16] Y.F. Hu, J. Zhou, P.-H. Yeh, Z. Li, T.-Y. Wei, Z.L. Wang, Adv. Mater. 22 (2010) 3327–3332.
[17] S. Liu, Q.L. Liao, S.N. Lu, Z. Zhang, G.J. Zhang, Y. Zhang, Adv. Funct. Mater. 26 (2016) 1347–1353.
[18] R.M. Yu, C.F. Pan, Z.L. Wang, Energy Environ. Sci. 6 (2013) 494–499.
[19] Y. Zhang, Z.L. Wang, Adv. Mater. 24 (2012) 4712–4718.
[20] Y. Ding, Y. Liu, S.M. Niu, W.Z. Wu, Z.L. Wang,J. Appl. Phys. 116 (2014), 154304.
[21] F. Xue, L.M. Zhang, X.L. Feng, G.F. Hu, F.R. Fan, X.N. Wen, L. Zheng, Z.L. Wang, Nano Res. 8 (2015) 2390–2399.
[22] L.M. Zhao, H. Li, J.P. Meng, Z. Li, InfoMat 2 (2020) 212–234.
[23] H. Li, C.C. Zhao, X.X. Wang, J.P. Meng, Y. Zou, S. Noreen, L.M. Zhao, Z. Liu, H. Ouyang, P.C. Tan, M. Yu, Y.B. Fan, Z.L. Wang, Z. Li,Adv. Sci. 6 (2019), 1801625.
[24] W. Jiang, H. Li, Z. Liu, Z. Li, J.J. Tian, B.J. Shi, Y. Zou, H. Ouyang, C.C. Zhao, L.M. Zhao, R. Sun, H.R. Zheng, Y.B. Fan, Z.L. Wang, Z. Li,Adv. Mater. 30 (2018), 1801895.
[25] L.M. Zhao, Q. Zheng, H. Ouyang, H. Li, L. Yan, B.J. Shi, Z. Li, Nano Energy 28 (2016) 172–178.
[26] Z. Li, Q. Zheng, Z.L. Wang, Z. Li,Research (2020), 8710686.
[27] Y. Zou, P.C. Tan, B.J. Shi, H. Ouyang, D.J. Jiang, Z. Liu, H. Li, M. Yu, C. Wang, X.C. Qu, L.M. Zhao, Y.B. Fan, Z.L. Wang, Z. Li, Nat. Commun. 10 (2019) 2695.
[28] J.Y. Sun, A.P. Yang, C.C. Zhao, F. Liu, Z. Li, Sci. Bull. 64 (2019) 1336–1347.
[29] Z.Y. Zhang, K. Yao, Y. Liu, C.H. Jin, X.L. Liang, Q. Chen, L.M. Peng, Adv. Funct. Mater. 17 (2007) 2478–2489.
[30] S.M. Sze, K.K. Ng. John wiley & sons 2006.
[31] S.J. Skinner, J.A. Kilner, Mater. Today 6 (2003) 30–37.
[32] Z. Zhang, C. Jin, X. Liang, Q. Chen, L.-M. Peng,Appl. Phys. Lett. 88 (2006), 073102.
[33] C.F. Pan, J.Y. Zhai, Z.L. Wang, Chem. Rev. 119 (2019) 9303–9359.
[34] Y. Zhang, Y. Liu, Z.L. Wang, Adv. Mater. 23 (2011) 3004–3013.
[35] Y. Zhang, Y. Leng, M. Willatzen, B. Huang, MRS Bull. 43 (2018) 928–935.
[36] L.M. Zhao, H. Li, J.P. Meng, A.C. Wang, P.C. Tan, Y. Zou, Z.Q. Yuan, J.F. Lu, C.F. Pan, Y.B. Fan, Y.M. Zhang, Y. Zhang, Z.L. Wang, Z. Li,Adv. Funct. Mater. (2019), 1907999.
[37] S. Mackowski, G. Prechtl, W. Heiss, F.V. Kyrychenko, G. Karczewski, J. Kossut,Phys. Rev. B 69 (2004), 205325.
[38] S.M. Niu, Y.F. Hu, X.N. Wen, Y.S. Zhou, F. Zhang, L. Lin, S.H. Wang, Z.L. Wang, Adv. Mater. 25 (2013) 3701–3706.
[39] Y.Y. Liu, P. Stradins, S.-H. Wei,Sci. Adv. 2 (2016), e1600069.
[40] B.D. Boruah, A. Mukherjee, S. Sridhar, A. Misra, ACS Appl. Mater. Interface 7 (2015) 10606–10611.
[41] W. Tian, T.Y. Zhai, C. Zhang, S.-L. Li, X. Wang, F. Liu, D.Q. Liu, X.K. Cai, K. Tsukagoshi, D. Golberg, Y. Bando, Adv. Mater. 25 (2013) 4625–4630.
[42] D. Gedamu, I. Paulowicz, S. Kaps, O. Lupan, S. Wille, G. Haidarschin, Y.K. Mishra, R. Adelung, Adv. Mater. 26 (2014) 1541–1550.
[43] Z. Zheng, L. Gan, J.B. Zhang, F.W. Zhuge, T.Y. Zhai,Adv. Sci. 4 (2017), 1600316.

[44] F. Teng, L.X. Zheng, K. Hu, H.Y. Chen, Y. Li, Z.M. Zhang, X.S. Fang, J. Mater. Chem. C 4 (2016) 8416–8421.
[45] W. Dai, X.H. Pan, S.S. Chen, C. Chen, W. Chen, H.H. Zhang, Z.Z. Ye, RSC Adv. 5 (2015) 6311–6314.
[46] C.-L. Hsu, Y.-D. Gao, Y.-S. Chen, T.-J. Hsu, ACS Appl. Mater. Interface 6 (2014) 4277–4285.
[47] B.D. Boruah, A. Mukherjee, S. Sridhar, A. Misra, ACS Appl. Mater. Interface 7 (2015) 10606–10611.